

## Controlling Chaos and Voltage Collapse using Layered Recurrent Network-based PID-SVC in Power Systems

I Made Ginarsa<sup>\*1</sup>, Agung Budi Muljono<sup>2</sup>, I Made Ari Nrartha<sup>3</sup>

Dept. of Electrical Engineering, Mataram University

Jln. Majapahit No. 62 Mataram, Telp/fax+62 370 636755

<sup>\*</sup>Corresponding author, e-mail: kadekgin@yahoo.com<sup>1</sup>, agungbm@yahoo.com<sup>2</sup>, ari.nrartha@gmail.com<sup>3</sup>

### Abstrak

Chaos dan voltage collapse muncul pada sistem tenaga listrik akibat gangguan energi pada beban kritis. Untuk mengatasinya maka dirancang PID-SVC yang berbasis-layered recurrent network (LRN). PID berbasis-LRN berfungsi untuk mengatasi chaos dan voltage collapse. Sementara itu, SVC berbasis-LRN berfungsi untuk mengatur tegangan beban. Hasil simulasi menunjukkan bahwa kontroler ini mampu mengatasi chaos dan voltage collapse pada sistem tenaga listrik. Lebih jauh lagi, kontroler ini mampu mengatur tegangan beban dengan cara mensuplai daya reaktif dari SVC. Respons dari kontroler yang diusulkan juga lebih baik dari PI-SVC.

**Kata kunci:** chaos, voltage collapse, PID-SVC, recurrent network, perbaikan tegangan

### Abstract

Chaos and voltage collapse occurred in critical power systems due to disturbing of energy. PID-SVC layered recurrent neural network-based (LRN-based PID-SVC) was proposed to solve these problems. The PID is used to control chaos and voltage collapse. Meanwhile, an SVC LRN-based is used to maintain the load voltage. By using the proposed controller, chaos and voltage collapse are able to suppress and maintain the load voltage around the setting value. When the maximum load is forced to load bus, the reactive power supplied by SVC, SVC additional voltage and load voltage are at the values of 0.1127,  $4.0095 \times 10^{-3}$  and 0.980010 pu, respectively. Furthermore, the proposed controller gives better response than PI-SVC controller.

**Keywords:** chaos, voltage collapse, PID-SVC, recurrent network, voltage maintain

### 1. Introduction

The Loading on electric power systems (EPS) was growth rapidly. On the other hand, the built of power plants and transmission line were very slow due to economical and environment reasons. Therefore, the existing EPS must be operated in critical condition on boundary of stability regions. Meanwhile, voltage collapse was found at the highest loading parameter existed on saddle node bifurcation (SNB) and voltage collapse analysis was done by using center manifold with static and dynamic approach [1]. The appeared of Hopf bifurcation (HB), chaos, crisis and voltage collapse before SNB were identified and classified in [2-3]. The appeared of HB in critical EPS was suppressed by using linear and nonlinear controllers in [4-5]. Chaos appeared in rotor speed, angle and voltage magnitude due to disturbing of energy (DE) [6]. Furthermore, chaotic behavior was observed in power systems and modelled using Elman recurrent neural networks (RNN). To validate the RNN model was compared to mathematical model, where the results of the both models were identical [7]. Controlling chaos and voltage collapse using continuation technique [8], ANFIS-based composite controller (CC)-SVC [9] and an additional PID-loop [10]. Artificial neural network (NN) was used in identification system and control application [11-13]. SVC controlled by NN was used to enhanced dynamic stability of EPS [14] and RNN was used as power system stabilizer in single machine [15].

Controlling chaos and voltage collapse using layered recurrent network (LRN)-based PID-SVC were focused in this research. This controller was chosen because it was trained in off-line mode by train data and easy to be implemented. This paper is organized as follows: Power system model is explained in Section 2. LRN-based PID-SVC controller design is detailed in

Section 3. Next, Chaos oscillation, voltage collapse and controller application, result and analysis are described in Section 4. Finally, the conclusion is provided in the last section.

Table 1. Power System Parameters

| $Y_0$         | $Y_m$    | $\theta_0, \theta_m$ | $V_0$    | $V_m$     |
|---------------|----------|----------------------|----------|-----------|
| 20.0          | 5.0      | -5.0                 | 1.0      | 1.0       |
| $P_m$         | $M$      | $D$                  | $T$      | $C$       |
| 1.0           | 1.0      | 0.3                  | 0.05     | 8.5       |
| $K_{p\omega}$ | $K_{pv}$ | $K_{q\omega}$        | $K_{qv}$ | $K_{qv2}$ |
| 12.0          | 0.3      | -0.03                | -2.8     | 2.1       |

All parameter values are in pu except for angle, which are in degrees.

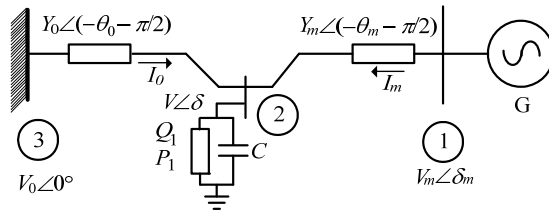


Figure 1. Three-bus power systems

### 2. Power System Model

A synchronous generator was connected to infinite bus therefore it was modeled by using a voltage ( $E'_{q0}$ ) behind a direct reactance ( $x'_d$ ). When the synchronous generator was operated in normal condition, the voltage magnitude was assumed as remaining constant at pre-disturbance [16]. The power systems supplied the balanced static load with saturation and the stator resistance were neglected. Then the armature current flowed from the generator to the load. Electrical torque was produced on stator winding due to the armature current. Therefore, the mechanical torque was produced by flux on the rotor winding. The rotor speed followed the synchronous speed in the normal operating condition. Meanwhile, when there was imbalanced energy in the generator, the rotor speed accelerated or decelerated. This condition can be expressed as a swing formula.

$$\Delta\dot{\omega} = 1/M (T_m - T_e - D\omega) \tag{1}$$

where  $T_m$ ,  $T_e$ ,  $\Delta\omega$ ,  $D$  and  $M$  are the mechanical torque, electrical torque, rotor speed deviation, damping constant and inertia constant, respectively.

In this research, the system was adopted from the work of Chiang et al. [1], as shown in Figure 1. This model represents the system as a synchronous generator that supplies power to an induction motor as local dynamic load with a shunt capacitor (Bus 2) connected by a weak tie line to an external system. By using parameters in Table 1 and put on the Eqs. (2-4) in [9,10] the parameters  $V'_0$ ,  $Y'_0$  and  $\theta'_0$  were obtained at the values of 2.5 pu, 8.0 pu and  $-0.209$ rad, respectively. Therefore, power system equations are expressed as Equation 2-5.

$$\dot{\delta}_m = \Delta\omega \tag{2}$$

$$\Delta\dot{\omega} = 1/M [-D\Delta\omega + P_m + V_m^2 Y_m \sin \theta_m + V_m V Y_m \sin(\delta - \delta_m - \theta_m)] \tag{3}$$

$$\dot{\delta} = 1/K_{q\omega} (-K_{qv}V - K_{qv2}V^2 + Q - Q_0 - Q_1) \tag{4}$$

$$\dot{V} = 1/TK_{q\omega}K_{pv} [K_{p\omega}K_{qv2}V^2 + (K_{p\omega}K_{qv} - K_{q\omega}K_{pv})V + K_{p\omega}(Q_0 + Q_1 - Q) - K_{q\omega}(P_0 + P_1 - P) + u(\Delta\omega)] \tag{5}$$

where the variables  $\delta_m$ ,  $\Delta\omega$ ,  $\delta$ ,  $V$ ,  $P$  and  $Q$  are the power angle, rotor speed deviation, voltage angle, voltage magnitude, real and reactive power, respectively. The variables  $P$  and  $Q$  are computed using Eqs. (6) and (7), respectively. The parameters  $P_1$ ,  $Q_1$  and  $D$  are the real load, reactive load and damping constant, respectively. The initial real ( $P_0$ ) and reactive ( $Q_0$ ) loads were taken at the values of 0.6 and  $j1.3$  pu, respectively. And the parameter  $u(\Delta\omega)$  was implemented as a control signal of power systems.

$$P = -V_0 V Y'_0 \sin(\delta + \theta'_0) - V_m V Y_m \sin(\delta - \delta_m + \theta_m) + (Y'_0 \sin \theta'_0 + Y_m \sin \theta_m) V^2 \tag{6}$$

$$Q = V_0 V Y'_0 \cos(\delta + \theta'_0) + V_m V Y_m \cos(\delta - \delta_m + \theta_m) - (Y'_0 \cos \theta'_0 + Y_m \cos \theta_m) V^2 \tag{7}$$

### 3. Layered Recurrent Neural Network-based PID-SVC Design

#### 3.1. PID Controller

PID controller has been extensively used by industries and researchers due to their simple structure, which can be easily understood and implemented. In this research, the main focus was to eliminate steady state error as well as to improve the dynamic response. The elimination of steady state error was realized by adding a pole at the origin using an integral controller. Furthermore, transient response was improved by the action of differential controller. The PID transfer function [17] is expressed as follow:

$$G(s) = k_p + \frac{k_i}{s} + k_d s \quad (8)$$

where  $G(s)$ ,  $k_p$ ,  $k_i$ ,  $k_d$  and  $s$  are the transfer function, proportional gain, integral gain, differential gain and Laplace operator, respectively. In this training stage, the  $P$ ,  $I$  and  $D$  gains were taken at the values of 0.092, 0.0032 and 0.0058, respectively.

#### 3.2 Static Var Compensator (SVC)

Static var compensator was shunt-connected static generator and/or absorber whose output was varied so as to control specific parameter of a power system. The term static was used to indicate that SVC has without any moving or rotating component [16: 693]. Let us start with SVC that was applied at bus  $k$ , and the reactive power was injected to bus  $k$

$$Q_k = V_k^2 B_{SVC} \quad (9)$$

where  $B_{SVC} = B_c - B_l$ ,  $B_{SVC}$ ,  $B_c$  and  $B_l$  are the SVC, capacitive and inductive susceptances, respectively. Then, dynamic equation of SVC is written as follow [18]:

$$\Delta \dot{B}_{SVC} = \frac{1}{t_{SVC}} \left[ \left( 1 - \frac{t_{v1}}{t_{v2}} \right) \Delta V_{r-SVC} - \Delta B_{SVC} - \frac{k_v t_{v1}}{t_{v2}} \Delta V_{t-SVC} \right] + \frac{k_v t_{v1}}{t_{v2} t_{SVC}} (\Delta V_{SS-SVC} + V_{ref}) \quad (10)$$

where  $t_{SVC}$ ,  $t_{v1}$ ,  $t_{v2}$ ,  $k_v$ ,  $V_{SS-SVC}$ ,  $V_{r-SVC}$ ,  $V_{t-SVC}$  and  $V_{ref}$  are the SVC time constant, time constant 1, time constant 2, SVC gain, SVC voltage at steady state, difference of reference and SVC voltage, difference of terminal and SVC voltage and reference voltage, respectively. In this training stage, the parameter values of SVC for the  $t_{SVC}$ ,  $t_{v1}$ ,  $t_{v2}$  and  $k_v$  were 70.0, 3.073-21.79, 400.0 and 30.0, respectively. The reference voltage was taken at the value of 0.98 pu.

#### 3.3. Layered Recurrent Network (LRN) Design Processes

A detailed method of LRN-based PID-SVC design is presented as follows:

1. Selection of input-output variables: The rotor speed deviation ( $\Delta\omega$ ) and its derivative ( $\Delta\dot{\omega}$ ) were chosen as the input of LRN-based PID. The output was the control signal ( $cs$ ). Meanwhile, the voltage angle ( $\delta$ ) and voltage magnitude ( $V$ ) were chosen as the input of the LRN-based SVC. And the output was the SVC susceptance ( $B_{SVC}$ ).
2. Architectures of LRN-based PID and SVC were built using three recurrent layers and a feed forward layer. First layer (Layer1) was consist of ten neurons, input weight ( $w_{11}$ ), recurrent weight1 ( $w_{12}$ ), bias ( $b_1$ ) and tangent sigmoid activation function (tansig). Second layer (Layer2) was consist of ten neurons, input weight ( $w_{21}$ ), recurrent weight1 ( $w_{22}$ ), bias ( $b_2$ ) and tangent sigmoid activation function (tansig). Third layer consist of a neuron, input weight3 ( $w_{31}$ ), recurrent weight1 ( $w_{32}$ ), bias ( $b_3$ ) and tangent sigmoid activation function (tansig). And, fourth layer consist of a neuron, input weight ( $w_{41}$ ), bias ( $b_4$ ) and linear activation function (purelin).
3. In this training process, the data matrix with  $2 \times 6000$  for input data,  $1 \times 6000$  for target data and in 100 epochs were used. Gradient descent backpropagation with adaptive learning rate (traingdx) and mean squared error (MSE) [19] were used for learning function and test performance function, respectively.
4. Furthermore, the architectures of LRN-based PID and SVC were formed by using [10 10 1 1] LRN. The architectures of the LRN are shown in Figures 2 and 3 for the LRN-PID and LRN-SVC, respectively. Where the parameter of the input weight4 ( $w_{41}$ ) were at the values of

-2.5068 and -0.8979 for LRN-PID and LRN-SVC, respectively. The bias4( $b_4$ ) parameters were at the values of 1.0397 and -0.2531 for LRN-PID and LRN-SVC, respectively.

5. After the training process was completed and the parameters of the LRN-PID and LRN-SVC were obtained, then the proposed controller was applied to power systems. The power systems with the proposed controller is shown in Figure 4.

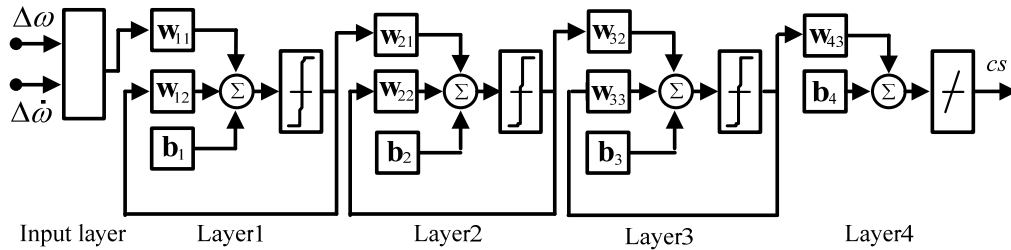


Figure 2. Architecture of PID-LRN with 10-10-1-1 layers.

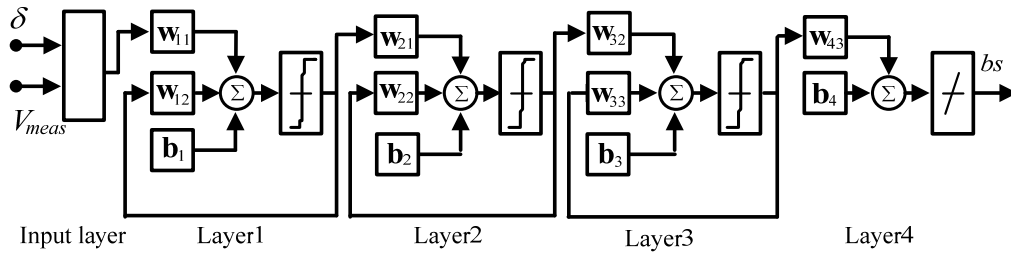


Figure 3. Architecture of SVC-LRN with 10-10-1-1 layers.

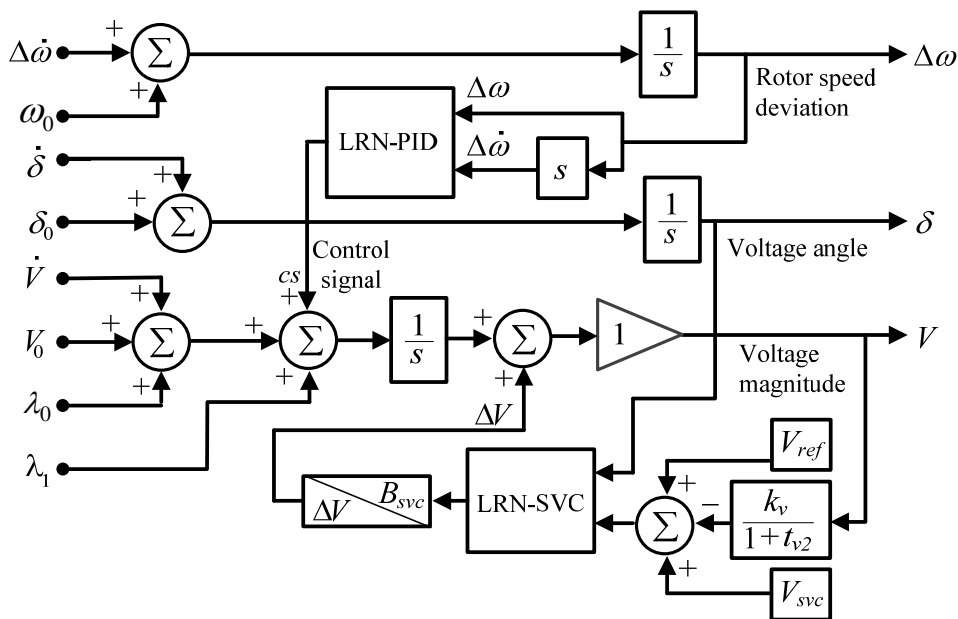


Figure 4. LRN-based PID-SVC controller was applied to power systems.

#### 4. Results and Analysis

In order to demonstrate the performance of the LRN-based PID-SVC to control chaos and voltage collapse in power systems, the systems were examined using Matlab/Simulink 7.9.0.529 on an Intel Core 2 Duo E6550 233 GHz PC computer.

##### 4.1 Power Systems Without Control Device

Power systems without any control device are very vulnerable, especially when these systems are operated in critical loading. Figure 5 shows chaotic oscillation of power systems when they were operated on initial condition ( $x_0$ ) at the value of [0.2 1.6700529800344 0.3 0.97]. In this operation, the load voltage magnitude ( $V$ ) was nonlinearly oscillated in the range of 0.82 - 1.12 pu. Therefore, Figure 6 shows the voltage collapse mechanism occurred at time of 442.315 s when power systems were operated at initial condition [0.2 1.2 0.3 0.97] and critical loading at the value of  $j10.898$  pu. Chaos and voltage collapse phenomena are serious problems in power system operation. Blackout phenomenon will occur at the overall of power systems if they are not able to control properly. To overcome chaos and voltage collapse problems, it is decided to use LRN-based PID-SVC (proposed controller) in power systems. The performance of the proposed controller is analyzed in the next section.

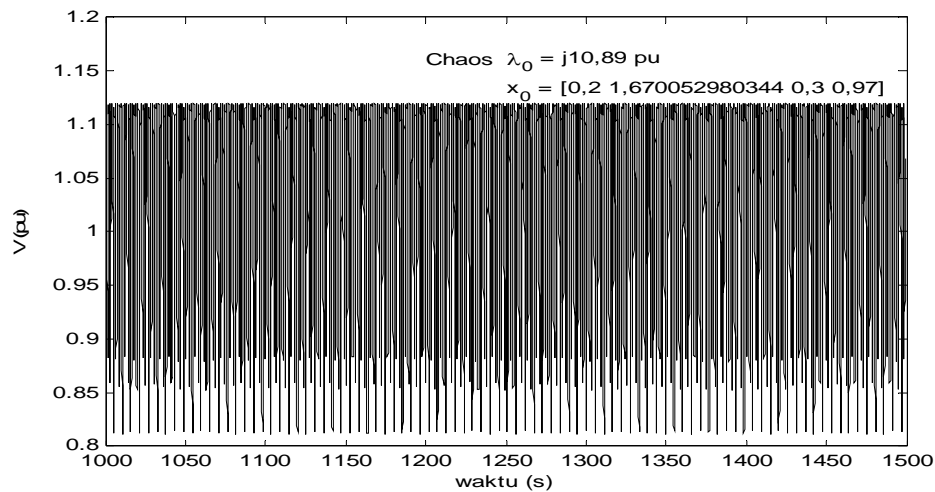


Figure 5. Chaos occurred in power systems

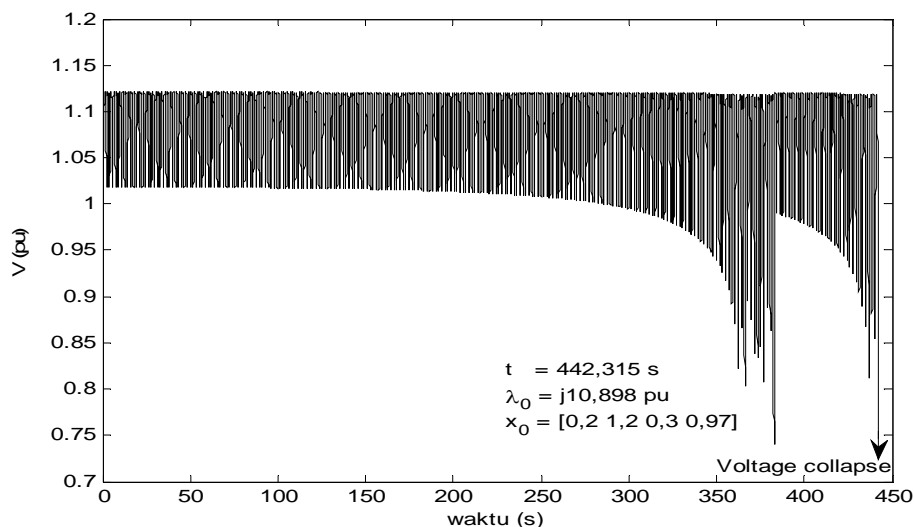


Figure 6. Voltage collapse mechanism of power systems when operated in critical loading.

**4.2. Power Systems with LRN-based PID-SVC Application**

First Scenario, power systems were equipped by LRN-based PID. In this scenario, both chaos and voltage collapse were adequate to suppress in power systems. However, performance of the controller was not good enough. The voltage magnitude ( $V$ ) was not able to maintain at setting value and the voltage magnitude was still varied according to load value at the load bus. Figure 7 shown that the voltage magnitude was at the value of 0.98 pu when the additional reactive load at the value of  $j0.0$  pu. Furthermore, the voltage magnitude was decreased to 0.9743, 0.9662, 0.9613 and 0.9522 pu when the additional reactive load was forced at the values of  $j0.01$ ,  $j0.02$ ,  $j0.03$  and  $j0.04$  pu, respectively. The voltage magnitude was at a low value when a high loading. On the contrary, the voltage magnitude at a high value when the loading was at a low value. In order to maintain the voltage magnitude at a setting value therefore LRN-based PID was equipped by LRN-based SVC. Performance of the proposed controller was evaluated in the next scenario

Second Scenario: LRN-based PID-SVC (proposed controller) was applied to power systems and load bus was forced by using four additional reactive loads at the values of  $j0.01$ ,  $j0.02$ ,  $j0.03$  and  $j0.04$  pu. Simulation results of this scenario are shown Figure 8-12 and listed in Table 2.

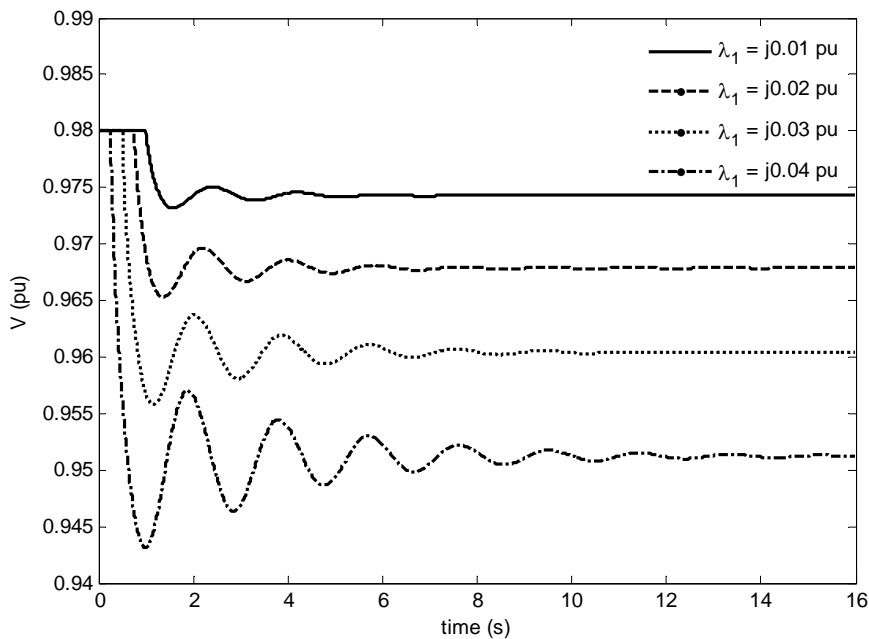


Figure 7. Power systems were equipped by LRN-based PID and forced by reactive load at the values of  $j0.01$ ,  $j0.02$ ,  $j0.03$  and  $j0.04$  pu.

Table 2. Simulation results of power systems when additional loads were forced to load bus at the values of  $j0.01$ ,  $j0.02$ ,  $j0.03$  and  $j0.04$  pu.

| $\lambda_1(\times j \text{ pu})$ | $V_{no}(\text{pu})$ | $B_{svc}(\times j \text{ pu})$ | $Q_{svc}(\times j \text{ pu})$ | $\Delta V(\times 10^{-3} \text{ pu})$ | $V(\text{pu})$ |
|----------------------------------|---------------------|--------------------------------|--------------------------------|---------------------------------------|----------------|
| 0.01                             | 0.9743              | 0.0173                         | 0.0166                         | 0.5853                                | 0.980038       |
| 0.02                             | 0.9671              | 0.0396                         | 0.0380                         | 1.3431                                | 0.980047       |
| 0.03                             | 0.9573              | 0.0733                         | 0.0700                         | 2.4828                                | 0.980033       |
| 0.04                             | 0.9427              | 0.1183                         | 0.1127                         | 4.0095                                | 0.980010       |

Figure 8 shows responses of PID, PI-SVC and the proposed controller. When power systems were equipped by PID controller without SVC, then an additional load was forced at time  $t_1(0.5 \text{ s})$ , voltage magnitude was decreased and oscillated in around 6.3 s.

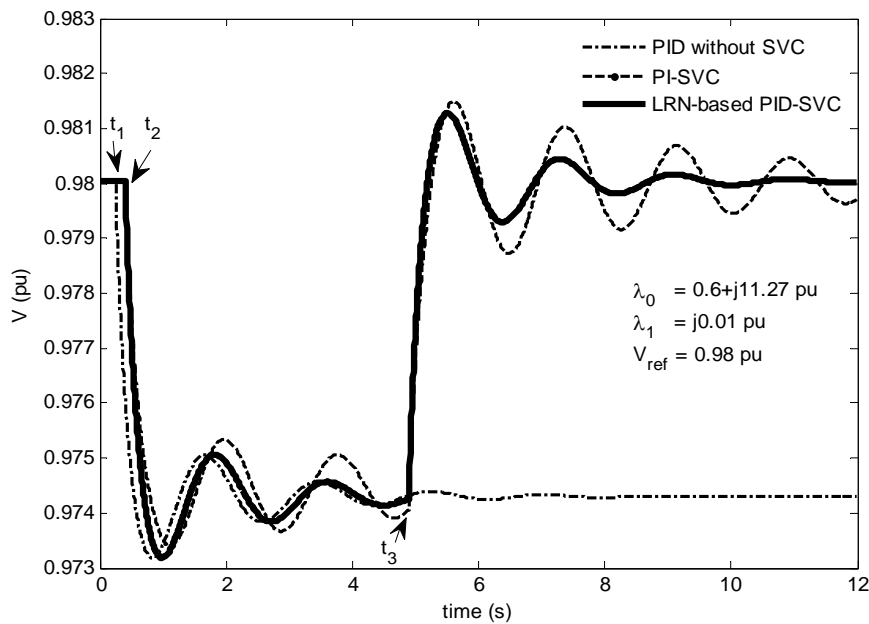


Figure 8. Comparison of PID, PI-SVC and LRN-based PID-SVC responses when additional load was forced to power systems at time  $t_1$ ;  $t_2$  and the SVC was switched on at time  $t_3$ .

Furthermore, the voltage magnitude was damped and settled at the value of 0.9746 pu. When power systems were equipped by PI-SVC, an additional load was forced at ( $t_2 = 0.6$  s). The voltage magnitude was decreased and oscillated with minimum voltage at around 0.9732 pu. At  $t_3 = 4.5$  s the SVC was fired and the voltage magnitude was increased and oscillated with maximum voltage was obtained at the value of 0.9815 pu. Furthermore, the voltage magnitude was damped and settled at the value of 0.98 pu and the settling time more than 12 s. When power systems were equipped by the proposed controller (LRN-based PID-SVC), an additional load was also forced at  $t_2$  and the voltage magnitude also decreased around 0.9743 pu. At  $t_3$  the SVC was switched on and the voltage magnitude was increased to maximum voltage at the value of 0.9805 pu. Moreover, the voltage magnitude was oscillated and damped undergo to magnitude at 0.98 pu and settling time at time of 9.6 s. From Figure 8 we can see that the response of the proposed controller was better than the other controller where maximum voltage and settling time of the proposed controller were obtained less than the other.

### 4.3. Power Systems Disturbed by Variation Additional Load

#### a. Power system disturbed by additional load at $j0.01$ pu

In this scenario, the proposed controller was applied to power systems and the power systems were forced by using additional load at the value of  $j0.01$  pu. The responses of the proposed controller and PI-SVC were compared in order to validate of the both responses. At first time, the power systems supplied on initial loading at the value of  $0.6 + j11.27$  pu. Simulation results are shown in Figure 9 and listed in Table 2. Figure 9 shows the response of the voltage magnitude when additional load  $j0.01$  pu was forced to load bus at  $t_4$  (15 s). In this operation, the balance of reactive power in the network was disturbed by the additional load and the voltage magnitude became to decrease at the value of 0.9743 pu. Furthermore, at  $t_5$  (25 s) an SVC device was switched on and the voltage magnitude increased again to the value of 0.980038 pu. In this operation, SVC susceptance ( $B_{svc}$ ) and reactive power supplied from SVC to network ( $Q_{svc}$ ) were obtained at the values of  $j0.0173$  and  $j0.0166$  pu, respectively. And, the SVC additional voltage ( $\Delta V$ ) was obtained at the value of  $0.5853 \times 10^{-3}$  pu.

Figure 9 shows that the voltage magnitude responses of PI-SVC controller was more oscillated than the response of the voltage magnitude of the proposed controller. And, the settling time of the voltage magnitude of PI-SVC controller was longer than the voltage magnitude of the proposed controller. The difference of the both responses were very clear in interval 0-15 s. The response of the proposed controller is better than PI-SVC controller.

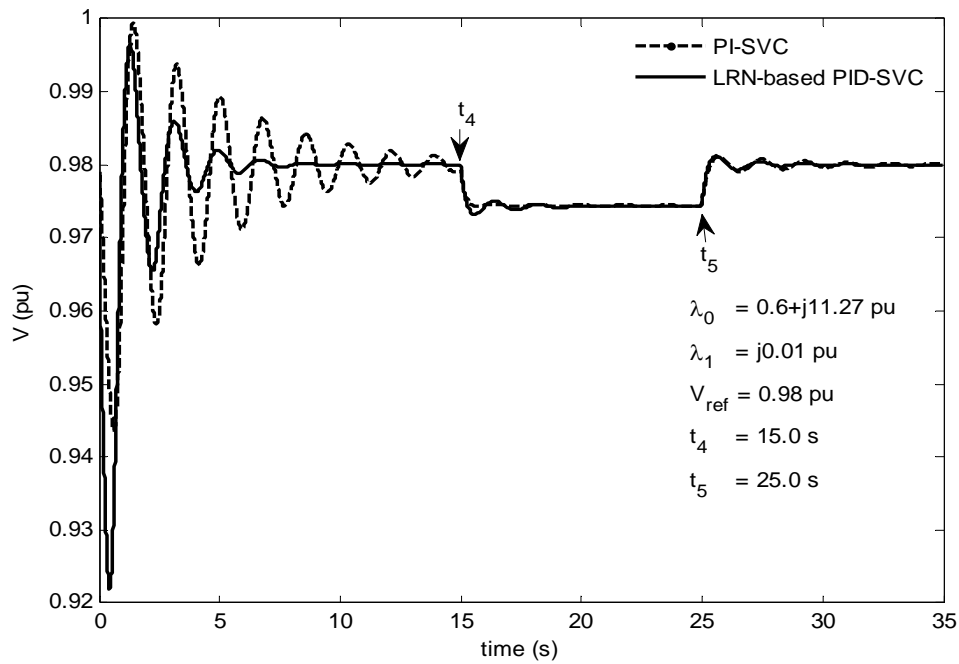


Figure 9. Responses of PI-SVC and LRN-based PID-SVC when the  $j0.01$ pu was forced to load bus at time  $t_4$  then the SVC was switched on at time  $t_5$ .

b. Power systems disturbed by additional load at  $j0.02$  pu

Figure 10 and Table 2 show the simulation results of power systems. Additional load at  $j0.01$  pu was forced at time  $t_4$  (10 s). In this operation the network was deficit of reactive power then the voltage magnitude was decreased until  $t_5$  (15 s).

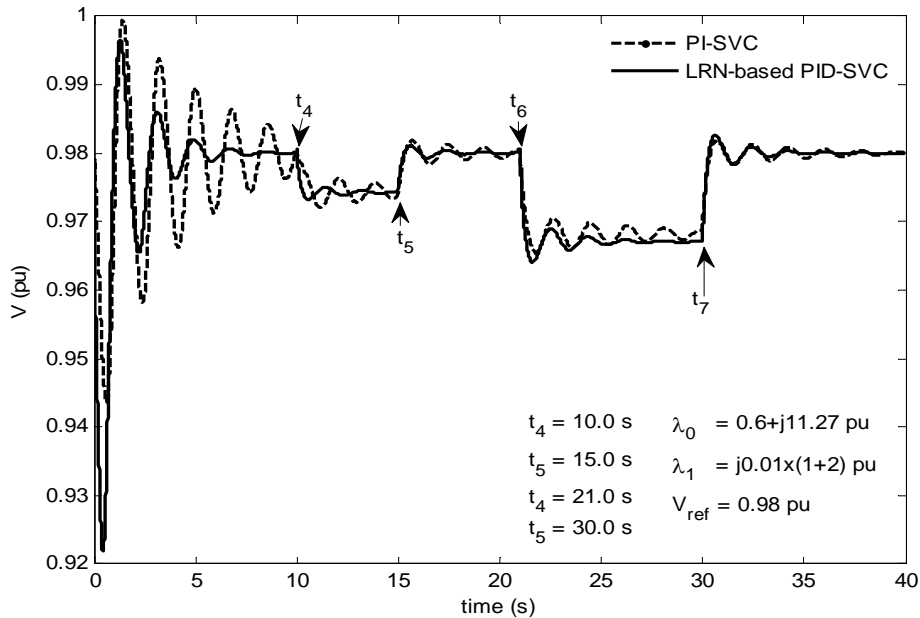


Figure 10. Responses of PI-SVC and LRN-based PID-SVC when additional load at  $j0.01$  and  $j0.02$  pu were forced to load bus at time  $t_4; t_6$  and the SVC was switched on at time  $t_5; t_7$ .



In order to increase the load voltage to the setting value, it was needed to switch on the SVC device at  $t_5$ . The reactive power was injected from SVC to the network at the value of  $j0.0166$  pu. By using this reactive power then the voltage magnitude was increased to the setting value until  $t_6$  (21 s). Next, the additional load at  $j0.02$  pu was forced at time  $t_6$ , at this moment the load voltage decreased to the value of  $0.9671$  pu until  $t_7$  (30 s). And, the SVC susceptance ( $B_{svc}$ ) and reactive power injected from SVC to networks ( $Q_{svc}$ ) were increased to the values of  $j0.0396$  pu and  $j0.0380$  pu, respectively. In this operation, the SVC supplied the additional voltage to the network ( $\Delta V$ ) at the value of  $1.3431 \times 10^{-3}$  pu. Finally, the load voltage ( $V$ ) was able to increase at the value of  $0.980047$  pu. The increased of load forced to power systems so that the SVC susceptance, SVC reactive power supplied and SVC additional voltage also increased.

PI-SVC and LRN-based PID-SVC (proposed controller) responses were compared in Figure 10. It is shown that the PI-SVC response was more oscillated than the proposed controller. Meanwhile, the proposed controller gave settling time more rapid than the PI-SVC controller. Moreover, the proposed controller gives better response than the PI-SVC controller.

#### c. Power systems disturbed by additional load at $j0.03$ pu

The power systems equipped by the controller were tested using larger additional loads at the values of  $j0.01$ ,  $j0.02$  and  $j0.03$  pu. Simulation results are shown in Figure 11 and listed in Table 2. At first time, the power systems were operated in an initial load at  $0.6 + j11.27$  pu. The responses of both controllers are shown in Figure 11 in interval  $0-t_4$  (10 s). The additional load  $j0.01$  was forced to load bus and the voltage magnitude was decreased until  $t_5$  (15 s). At  $t_5$ , the SVC was switched on. Therefore, the SVC supplied reactive power to network and the voltage magnitude was increased to around the setting value until  $t_6$  (20 s). The additional load at  $j0.02$  pu was forced to the load bus at  $t_6$  and the voltage magnitude decreased immediately to  $0.9671$  pu. In order to increase the voltage magnitude to around the setting value ( $0.98$  pu) again, the SVC susceptance ( $B_{svc}$ ) must be increased at the value of  $j0.0396$  pu at  $t_7$  (28.0 s). And, the reactive power supplied by the SVC to the network ( $Q_{svc}$ ) increased also at the value of  $j0.0380$  pu. The voltage magnitude ( $V$ ) stayed at around the setting value until  $t_8$  (35 s). Next, a larger additional load at  $j0.03$  pu was forced to the load bus at  $t_8$  and the voltage magnitude decreased to a lower value ( $0.9573$  pu) until  $t_9$  (49 s). Finally, the SVC susceptance was increased to the value of  $j0.0733$  pu at time  $t_9$ , and reactive power support from the SVC to the network increased also at the value of  $j0.0700$  pu. In this operation, the SVC produced additional voltage ( $\Delta V$ ) at  $2.4828 \times 10^{-3}$  pu in order to support the load voltage ( $V$ ) achieved the setting value at  $0.980033$  pu.

According to results in Table 2, it is shown that the additional load was increased so that the SVC susceptance, reactive power supplied from the SVC and SVC additional voltage should be increased in order to maintain the voltage magnitude stayed around the setting value. Meanwhile, from Figure 11 we can see that voltage magnitude response of PI-SVC is more oscillated than the voltage magnitude response of the proposed controller. And, the voltage magnitude response of PI-SVC is more difficult to achieve equilibrium point than the response of the proposed controller. From these responses it is shown that the performance of the proposed controller is better than the PI-SVC.

#### d. Power systems disturbed by additional load at $j0.04$ pu

Furthermore, power systems equipped by controller were forced by additional load at the values of  $j0.01$ ,  $j0.02$ ,  $j0.03$  and  $j0.04$  pu. The voltage magnitude ( $V$ ) response is shown in Figure 12 and complete results of simulation are listed in Table. At first time, the additional load  $j0.01$  pu was forced to load bus at time  $t_4$  (9 s) and the voltage magnitude was decreased to the value of  $0.9743$  pu until time  $t_5$  (14 s).

Next, at time  $t_5$  the SVC was switched on and connected to the network. The SVC susceptance was existed at the value of  $j0.0173$  pu and the SVC supplied reactive power to the network at the value of  $j0.0166$  pu. The voltage magnitude was increased to around the setting value, due to reactive power support from the SVC until  $t_6$  (18 s). Next, the additional load ( $j0.02$  pu) was forced at load bus at time  $t_6$  and voltage magnitude was decreased and stayed until  $t_7$  (24 s). Then, the SVC susceptance was increased and made the voltage magnitude also increased to around the setting value until  $t_8$  (29 s).

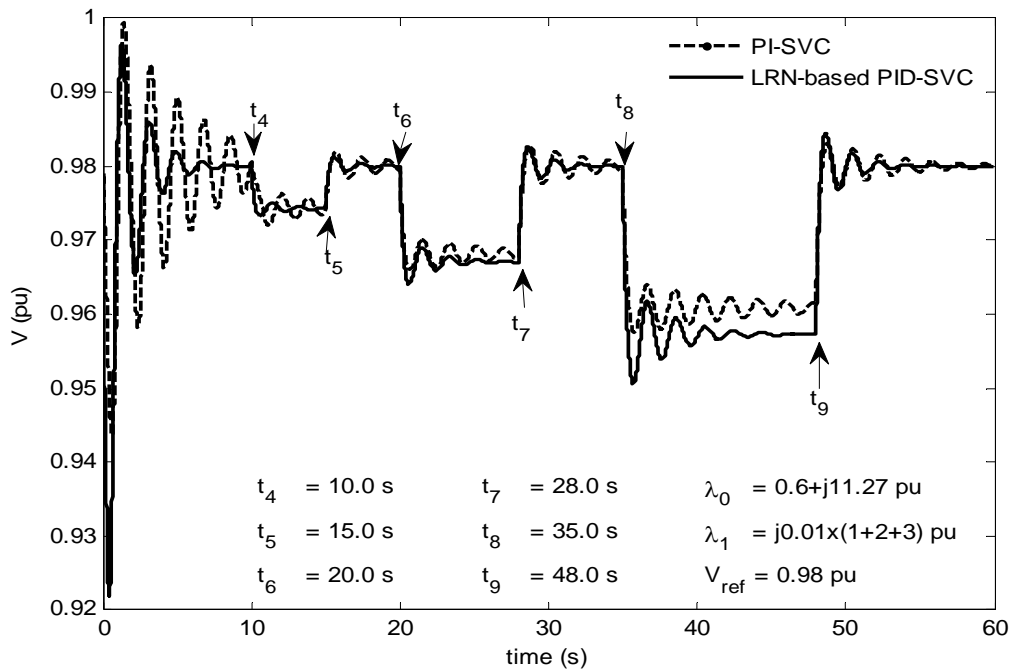


Figure 11. Responses of both controllers when the loads at  $j0.01 \times (1+2+3)$  pu were forced to load bus, then the SVC was switched on and increased the SVC susceptance.

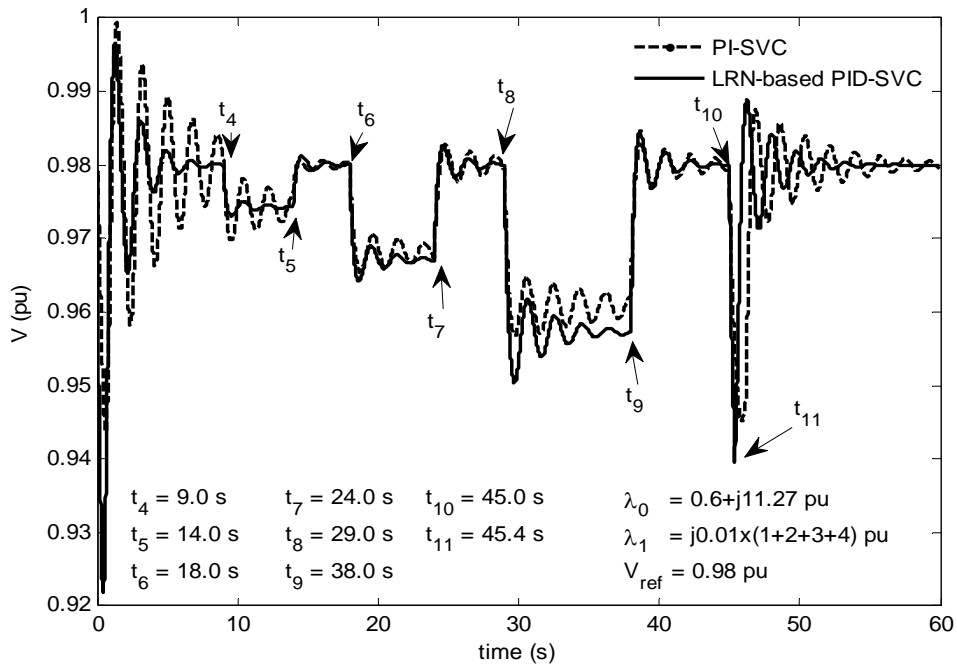


Figure 12. Dynamical Responses of both controllers when the loads at  $j0.01 \times (1+2+3+4)$  pu were forced, then the SVC was switched on and increased the SVC susceptance.

At time  $t_8$ , the additional load ( $j0.03$  pu) was forced to load bus. And, the voltage magnitude was decreased again due to deficit of reactive power in the network until time  $t_9$  (35 s). Next, at  $t_9$  the SVC susceptance was increased to support reactive power to the network and the voltage

magnitude increased to the setting value until time  $t_{10}$  (35 s). The maximum additional load at the value of  $j0.04$  pu was forced to the load bus at  $t_{10}$  and the voltage magnitude decreased immediately to 0.9427 pu. Finally, the SVC susceptance was increased to the value of  $j0.1183$  pu at time  $t_{11}$  (45.4 s). At this SVC susceptance, the SVC supplied reactive power to the network at the value of  $j0.1127$  pu. The additional voltage from the SVC to networks ( $\Delta V$ ) and the voltage magnitude were at the values of  $4.0095 \times 10^{-3}$  and 0.980010 pu, respectively.

## 5. Conclusion

The grown up of load demand on power systems was rapidly. Meanwhile, power plant and transmission line being built was slow due to economical and environmental constraint. This condition makes the existing power systems were operated on heavy loading near the limit of stability. When power systems are operating near the limit of stability that makes the nonlinear phenomena appearing in power systems such as chaos and voltage collapse. Therefore, LRN-based PID-SVC is proposed to control chaos and voltage collapse in power systems. LRN-based PID is used to suppress chaos and voltage collapse. Meanwhile, LRN-based SVC is used to regulate and maintain the load voltage. Simulation results show that the proposed controller is able to control chaos and voltage collapse. Moreover, the proposed controller is able to maintain the voltage magnitude at the setting value by controlling the SVC susceptance. The maximum loading that can be covered handled by the proposed controller is  $j0.04$  pu. And, the SVC susceptance is obtained at the value of  $j0.1183$  pu. In this operation, the SVC supplied the reactive power to the network and the SVC additional voltage are obtained at the values of  $j0.1127$  and  $4.0095 \times 10^{-3}$  pu, respectively. Furthermore, voltage magnitude response of the proposed controller is better than voltage magnitude response of the PI-SVC controller.

## References

- [1] Chiang HD, Dobson I, Thomas RJ. On Voltage Collapse in Electric Power Systems, *IEEE Transactions on Power Systems*. 1990; 5(2): 601-611.
- [2] Ajarapu V, Lee B. Bifurcation Theory and Its Application to Nonlinear Dynamical Phenomena in an Electrical Power System. *IEEE Transactions on Power Systems*. 1992; 7(1): 424-431.
- [3] Chiang HD, Liu CW, Varaiya PP, Wu FF, Lauby MG. Chaos in a Simple Power System. *IEEE Transactions on Power Systems*; 1993; 8(4): 1407-1417.
- [4] Wang HO. Control of Bifurcation and Routes to Chaos in Dynamical System. PhD Thesis. University of Maryland; 1993.
- [5] Wang HO, Abed EH, Hamdan AMA. Bifurcations, Chaos, and Crises in Voltage Collapse of a Model Power System. *IEEE Transactions on Circuits and Systems 1: Fundamental Theory and Applications*. 1994; 41(3): 294-302.
- [6] Ginarsa IM, Soeprijanto A, Purnomo MH. Implementasi Model Klasik untuk Identifikasi Chaotic dalam Sistem Tenaga Listrik Akibat Gangguan Energi. Seminar on Intelligent Technology and Its Applications (SITIA). Surabaya. 2008: 508-513.
- [7] Ginarsa IM, Soeprijanto A, Purnomo MH. Modelling of Chaotic Behavior in Power Systems Using Recurrent Neural Networks. International Conference on Advanced Computational Intelligence and Its Application (ICACIA). Jakarta. 2008: 51-56.
- [8] Subramanian DP, Devi RPK, Saravanaselvan R. A new algorithm for analysis of SVC's impact on bifurcation chaos and voltage collapse in power systems. *International Journal of Electrical Power and Energy Systems*. 2011; 33(5): 1194-1202.
- [9] Ginarsa IM, Soeprijanto A, Purnomo MH. Controlling chaos and Voltage Collapse using an ANFIS-based Composite Controller-Static Var Compensator in Power Systems. *International Journal of Electrical Power and Energy Systems*. 2013; 46: 79-88.
- [10] Ginarsa IM, Soeprijanto A, Purnomo MH, Syafaruddin, Hiyama T. Improvement of Transient Voltage Responses using an Additional PID-loop on an ANFIS-based Composite Controller-SVC (CC-SVC) to Control Chaos and Voltage Collapse in Power Systems. *IEEJ Transactions on Power and Energy (Section B)*. 2011; 131(10): 836-848.
- [11] Narendra KS, Mukhopadhyay S. Adaptive Control Using Neural Networks and Approximate Models. *IEEE Transactions on Neural Networks*. 1997; 8(3): 475-485.
- [12] Levin AU, Narendra KS. Control of Nonlinear Dynamical Systems Using Neural Networks—Part II: Observability, Identification and Control. *IEEE Transactions on Neural Networks*. 1996; 7(1): 30-42.
- [13] Narendra KS, Parthasarathy K. Identification and Control of Dynamical Systems Using Neural Networks. *IEEE Transactions on Neural Networks*. 1990; 1(1): 4-27.

- 
- [14] Harikrishna D, Srikanth NV. Dynamic stability enhancement of power systems using neural-network controlled static-compensator. *Telkomnika*. 2012; 10(1): 9-16.
- [15] Aribowo W. Stabilisator sistem tenaga listrik berbasis jaringan syaraf tiruan berulang untuk sistem mesin tunggal. *Telkomnika*. 2010; 8(10): 65-72.
- [16] Kundur P. Power System Stability and Control. EPRI. New York: McGraw-Hill. 1994.
- [17] Mukherjee V, Ghoshal SP. Intelligent Particle Swarm Optimized Fuzzy PID Controller for AVR System. *Electric Power Systems Research*. 2008; 77(12): 1689-1698.
- [18] Zhang XP, Rehtanz C, Pal B. Flexible AC Transmission Systems: Modeling and Control. Berlin: Springer-Verlag. 2006.
- [19] MATLAB Version 7.9.0.529 (2009b): The Language of Technical Computing, 2009, The Matworks Inc.